JACS
JOURNAL OF THE AMERICAN CHEMICAL SOCIETY

Communication

pubs.acs.org/JACS

Electrochemistry of Aqueous Pyridinium: Exploration of a Key Aspect of Electrocatalytic Reduction of CO_2 to Methanol

Yong Yan, Elizabeth L. Zeitler, Jing Gu, Yuan Hu, and Andrew B. Bocarsly*

Department of Chemistry, Princeton University, Princeton, New Jersey 08544, United States

Supporting Information

ABSTRACT: The mechanism by which pyridinium ($pyrH^+$) is reduced at a Pt electrode is a matter of recent controversy. The quasireversible cyclic voltammetric wave observed at −0.58 V vs SCE at a Pt electrode was originally proposed to correspond to reduction of $pyrH^+$ to pyridinyl radical ($pyrH^•$). This mechanistic explanation for the observed electrochemistry seems unlikely in light of recent quantum mechanical calculations that predict a very negative reduction potential (−1.37 V vs SCE) for the formation of $pyrH^•$. Several other mechanisms have been proposed to account for the discrepancy in calculated and observed reduction potentials, including surface adsorption of $pyrH^•$, reduction of $pyrH^+$ by two electrons rather than one, and reduction of the $pyrH^+$ proton to a surface hydride rather than a π-based radical product. This final mechanism, which can be described as inner-sphere reduction of $pyrH^+$ to form a surface hydride, is consistent with experimental observations.

Electrochemical reduction of CO_2 with pyridinium ($pyrH^+$) as a catalyst has been reported to occur at low overpotentials to form formic acid and methanol at various interfaces including Pt,[1] Pd,[2] p-GaP,[3] iron pyrite,[4] and Pt/C-TiO_2.[5] We previously suggested that the electrocatalytic mechanism involved a mediated charge-transfer (CT) process in which $pyrH^+$ is reduced at an electrode surface via a one-electron ($1e^-$) CT, followed by reaction of the electrogenerated pyridinyl radical ($pyrH^•$) with CO_2 to form a carbamate radical adduct (Scheme 1).[1] This proposal has been used to explain the quasireversible cyclic voltammetry (CV) of $pyrH^+$ at a Pt electrode (see Figure 1), which occurs with a standard redox potential of −0.58 V vs SCE, consistent with literature reports of electroanalytical reduction of $pyrH^+$ in the absence of CO_2.[6] A mechanism that involves $1e^-$ reduction of the $pyrH^+$ π-system followed by a second electron transfer (ET) to the carbamate radical (Scheme 1) is consistent with the scan-rate-dependent current enhancement observed in the CV of $pyrH^+$ under CO_2, as well as the first-order dependence of current on $pyrH^+$ and CO_2.[7] The proposed pyr-CO_2 radical carbamate intermediate was observed via vibrational spectroscopy in the gas-phase reaction of $CO_2^{•-}$ and pyr, supporting the reactivity suggested in Scheme 1.[8]

Keith and Carter recently provided computational access to the pK_a's and redox potentials of the short-lived $pyrH^•$ formed via electroreduction of various substituted $pyrH^+$'s in aqueous solution.[9] The pK_a for deprotonation of the $pyrH^•$ nitrogen in water was calculated to be ∼27; this was confirmed by an independent calculation by Musgrave.[10] Such a high pK_a makes deprotonation unfavorable, resulting in a high-energy transition state for formation of a carbamate radical intermediate. This is inconsistent with the low overpotential measured experimentally for $pyrH^+$-catalyzed CO_2 reduction at a Pt electrode. Additionally, the reduction potential of $pyrH^+/pyrH^•$ in solution was calculated to be −1.37 V vs SCE,[11] 800 mV more negative than the experimentally observed reduction potential at a Pt electrode. Other groups calculated similarly high reduction potentials for $pyrH^+$ to $pyrH^•$.[10,12] The discrepancy between these theoretical calculations and the experimentally observed redox potential at a Pt electrode calls into question the existence of $pyrH^•$ in solution.

Scheme 1. Pyridinium Reduction by One Electron, Forming the Pyridinyl Radical, Followed by Its Reaction with CO_2 To Form a Radical Carbamate

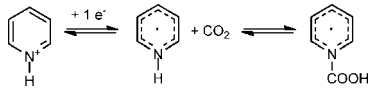

Several mechanisms for CO_2 reduction with $pyrH^+$ catalysis have been proposed given the discrepancies noted above. Possible mechanisms associated with initial CT to $pyrH^+$ include formation of 4,4′-bipyridine (bpy) from $pyrH^+$,[9] $2e^-$ reduction of $pyrH^+$ to form 1,4-dihydropyridine (DHP),[11] facilitated carbamate radical formation via a cyclic transition state utilizing bridging water molecules,[10] and reduction of CO_2 by a surface-confined platinum hydride (Pt-H) formed by reduction of the acidic $pyrH^+$ proton.[12b] Here we experimentally examine the proposed $pyrH^+$ reduction mechanisms. In addition to the carbamate-based mechanism that we previously hypothesized, another plausible mechanism for the observed electrocatalytic process on a Pt electrode proceeds through direct formation of Pt-H via inner-sphere reduction of $pyrH^+$.

Mechanism I: $pyrH^•$ as the Primary Reduction Product. Explicit experiments were conducted to detect the transient formation of $pyrH^•$ from $pyrH^+$ in aqueous and organic solvents. UV/vis and EPR spectroelectrochemistry were undertaken in an attempt to observe the π-radical. In situ electrochemical generation of radical species at a Pt electrode was consistently detected by EPR and UV/vis spectroscopy in aqueous solution at room temperature when 4,4′-bipyridinium was used as reactant (Figure S1). A π-radical-reduced cyanopyridine derivative was also observed spectroelectrochemically.[15] However, in parallel

Received: June 24, 2013
Published: August 23, 2013

   dx.doi.org/10.1021/ja4064052 | J. Am. Chem. Soc. 2013, 135, 14020−14023

experiments with $pyrH^+$, no evidence for the formation of $pyrH^\bullet$ was observed.

Separately, transient absorption spectroscopy detected reduction of bpy to 4,4′-bipyridinyl radical by excited $[Ru(bpy)_3]^{2+}$ ($Ru(III)/Ru(II)^* = -0.89$ V vs SCE). In contrast, no formation of $pyrH^\bullet$ was observed in the presence of $pyrH^+$ and excited $[Ru(bpy_3]^{2+}$ under the same conditions. Stern−Volmer quenching studies were applied using $pyrH^+$ or bpy as quencher and $[Ru(bpy)_3]^{2+}$ as luminophore in aqueous solution. A quenching rate constant $k_q \approx 2\times10^9$ $M^{-1}s^{-1}$ was obtained for bpy; however, negligible quenching was observed for $pyrH^+$.[16] This indicates a redox potential more negative than −0.89 V vs SCE for $pyrH^+/pyrH^\bullet$. Conversely, we observe that $pyrH^+$ does CT-quench $[Ir(ppy)_3]$ (ppy = 2-phenylpyridine) $Ir(IV)/Ir(III)^* = -1.73$ V vs SCE, excited-state lifetime $\tau = 1.9$ μs). A Stern−Volmer plot was obtained with $K_{sv} = 116$ M^{-1}, indicating $k_q \approx 10^8$ $M^{-1}s^{-1}$ for $pyrH^+$ quenching (Figure S2). The observed quenching requires a redox potential for $pyrH^+/pyrH^\bullet$ less negative than −1.73 V vs SCE. The spectroelectrochemical and quenching studies together with theoretical calculations imply that electrochemical generation of $pyrH^\bullet$ at −0.58 V vs SCE in aqueous solution is unlikely to occur via an outer-sphere process.

Mechanism II: Surface-Adsorbed $pyrH^+$ or $pyrH^\bullet$. Keith and Carter suggested that the free energy discrepancy between the calculated and observed reduction potentials might be associated with surface adsorption of $pyrH^\bullet$.[9] Similarly, Musgrave's group suggested that $pyrH^+$ adsorption on a Pt electrode could shift the reduction potential anodically relative to that of solution-based $pyrH^+$.[10] Strong adsorption manifests itself in CV as a wave with peak current (i_p) proportional to scan rate and, in the ideal limit, zero separation in oxidative and reductive peak potential. This wave can coexist with a diffusion-limited wave and in that case appears as either prepeaks (adsorbed product) or postpeaks (adsorbed reactant).[17] The primary reduction wave of $pyrH^+$ has i_p proportional to the square root of scan rate and limiting current (i_l) in rotating disk voltammetry (RDV) proportional to the square root of rotation rate, indicating a diffusion-limited reaction. But $pyrH^+$ reduction at a Pt electrode is more complex than a simple outer-sphere ET, as shown in Figure 1. At high scan rates (>200 mV/s), prepeak shoulders observed on the $pyrH^+$ wave suggest the presence of adsorptive processes in addition to the primary diffusive peak. These prefeatures are similar to those observed in other acid reductions, e.g. potassium hydrogen phthalate and acetic acid as well as reduction of protons from strong acids, indicating the prefeatures are not specific to pyr or its derivatives (Figure S3). Thus, selective adsorption of $pyrH^+$ must be ruled out as the source of the discrepancy.

Mechanism III: A $2e^-$ Reduced Product. If the reaction resulting in the observed voltammetry is not $1e^-$ reduction of $pyrH^+$ to $pyrH^\bullet$, but is in fact $2e^-$ reduction of $pyrH^+$ to DHP, then that would lead to a more positive reduction potential. Keith and Carter calculated the reduction potential of $pyrH^+$ to DHP to be −0.72 V vs SCE.[11] To identify the number of electrons transferred (n) in the observed reduction of $pyrH^+$, the i_p and i_l were evaluated. Both i_p and i_l are dependent on n and the diffusion coefficient (D) of the species being reduced (eqs 1 and 2). It is possible, using CV and RDV data, to calculate n and D of

$$i_p = (2.69 \times 10^5) n^{3/2} A C_O^* D^{1/2} \nu^{1/2} \quad (1)$$

$$i_l = 0.62 n F A C_O^* D^{2/3} \nu^{-1/6} \omega^{1/2} \quad (2)$$

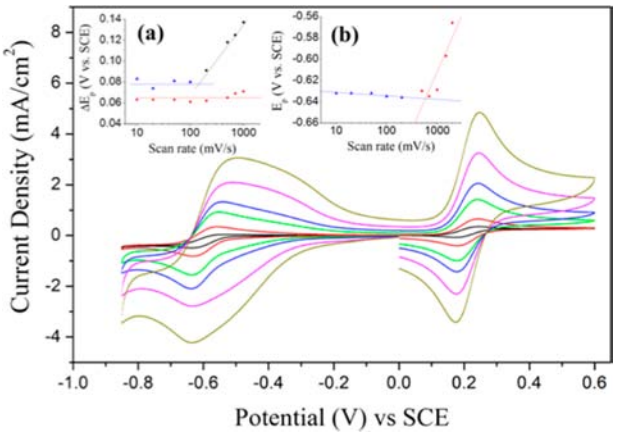

Figure 1. Scan rate dependence of $pyrH^+$ reduction on a Pt electrode in the presence of ferrocyanide (Fc) at 5, 20, 100, 200, 500, and 1000 mV/s; inset a plots peak separation vs log of scan rate for $pyrH^+$ (black) and Fc (red). $pyrH^+$ reduction showed a large diffusion-limited peak ($E_{1/2}$ = −0.58 V vs SCE) and prefeatures (∼ −0.4 V vs SCE) at scan rates above 100 mV/s, indicating a minor adsorptive process. For comparison, Fc ($E_{1/2}$ = 0.21 V vs SCE) exhibited reversible electrochemistry. The $pyrH^+$ reduction peak potential shifts more negative with scan rate above 500 mV/s, indicating quasireversibility. By Gileadi's method,[13] the heterogeneous ET rate constant was calculated to be 0.019 cm/s from the critical scan rate where peak potential begins to shift, 580 mV/s (inset b). This compares well to $k_{et} = 0.0078\pm0.0022$ cm/s calculated from digital simulation of the CV of $pyrH^+$.[7,14]

the analyte independent of an electrochemical standard in solution. Using plots of i_p vs $\nu^{1/2}$ and i_l vs $\omega^{1/2}$, values for n and D were calculated (Figure S4). For $pyrH^+$, $n = 0.8$ and $D = 2.1\times10^{-5}$ cm^2/s. Equations 1 and 2 assume a reversible process[17] that can be approximated for $pyrH^+$ in the absence of CO_2. $n = 0.8$ indicates a $1e^-$ transfer is occurring for the diffusion-limited peak, precluding $2e^-$ reduction to DHP. The value <1 can be attributed to the small current corresponding to the CV prefeatures observed (vide infra).

If DHP was produced as an intermediate, deuterium exchange at the pyr 4-position would be expected (Scheme 2). Exhaustive electrolysis at potentials near the peak of the voltammetric wave yields no exchange by ^1H NMR with either $pyrH^+$-d_5 electrolyzed in H_2O or H_5-$pyrH^+$ electrolyzed in D_2O.

Scheme 2. $pyrH^+$ Reduction to a DHP Intermediate in D_2O Electrolyte, Leading to Isotopic Scrambling at the 1 and 4 Positions

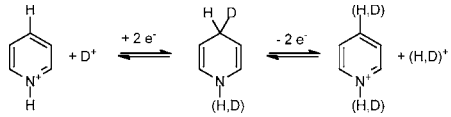

These observations exclude DHP as the product of voltammetric reduction. To investigate the reactivity of DHP with CO_2, DHP was synthesized[18] and reacted with CO_2, producing a gel. No reduced CO_2-derived products were detected in the gel. Upon acidification of the gel, CO_2 was released and detected by IR and GC, but again, no reduced products were detected by IR, GC, or NMR (Figure S5). This indicates DHP reacts with CO_2 as a strong base rather than as a reducing agent.

Keith and Carter pondered the possibility that the electrochemistry of $pyrH^+$ might involve transient formation of bpy

dx.doi.org/10.1021/ja4064052 | J. Am. Chem. Soc. 2013, 135, 14020−14023

Scheme 3. Formation of bpy from Oxidative pyr Coupling

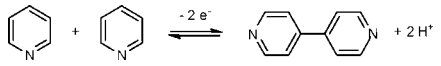

(Scheme 3), followed by rapid dissociation to regenerate $pyrH^+$ in solution. They calculated the reduction potential of bpy at a Pt electrode to be −0.58 V vs SCE and indicated that this may be the active species in the observed electrochemistry. Oxidative coupling of pyr to form bpy was reported in deareated and anhydrous nonprotic organic solvent with Pt particles as catalyst;[19] however, this coupling was not observed in aqueous solution. The quasireversibility of the CV data requires rapid cleaveage of a C−C bond to regenerate $pyrH^+$, implying formation of a transient bpy species is energetically untenable. Additionally, the lack of deuterium exchange of the $pyrH^+$ 4-position protons in electrolyses in D_2O argues against transient formation of bpy. Further, the reactivity of sterically hindered 4-*tert*-butylpyridinium would radically differ from that of $pyrH^+$ if the suggested coupling occurred, but this is not the case (see Figure 4). Finally, no oxidative $2e^-$ chemistry was detected in the CVs, ruling out electrochemical formation of bpy.

Mechanism IV: $pyrH^+$ as a Reagent for Pt-H Formation. The mechanisms discussed above focus on the $pyrH^+$ π-orbital as the electron acceptor. On a Pt electrode, the proton bound to the pyr nitrogen is reducible in its own right. The mechanistic possibility of proton reduction on a Pd electrode was previously considered when electrocatalytic $pyrH^+$ reduction of CO_2 was first reported.[2] Batista et al. recently provided theoretical support that hydride formation on the Pt(111) electrode surface might be important in the CO_2 reduction mechanism.[12b] The calculated redox potential for pyr-bound proton reduction (Scheme 4) is ∼ −0.7 V vs SCE, well within the range of theoretical error of what has been experimentally observed.

Scheme 4. Inner-Sphere Reduction of a $pyrH^+$-Bound Proton on a Pt Electrode To Form a Surface Hydride[12b]

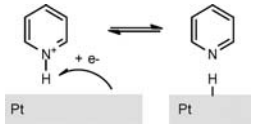

We examined this pathway experimentally by producing a Pourbaix diagram for $pyrH^+$ reduction. The CV of $pyrH^+$ on a Pt electrode was recorded with varying pH. It followed the expected behavior for weak acids[20] in that the half-wave potential ($E_{1/2}$) was stable at −0.58 V vs SCE when pH < pK_a and decreased with slope −59 mV when pH > pK_a (Figure 2). To maintain an observable $[pyrH^+]$ up to pH 8, the ratio of $pyrH^+$ to pyr was adjusted by adding pyr. The i_p was proportional to $[pyrH^+]$ at each pH as governed by the acid dissociation equilibrium. Further, when the pH was low enough for comparable $[pyrH^+]$ and $[H_3O^+]$ (pH 3, $[H_3O^+]$ = 1 mM), a wave representing H_3O^+ reduction at ∼ −0.4 V vs SCE was observed alongside that of $pyrH^+$ reduction at −0.58 V vs SCE (Figure 3). This wave continued to increase as pH decreased. This clearly indicates that the wave at −0.58 V vs SCE is due to $pyrH^+$ and not H_3O^+ reduction. The plateau redox potential at pH < pK_a indicated that reduction of $pyrH^+$ occurs in an electrochemical process that is unrelated to $[H_3O^+]$ in solution. As expected for a Pourbaix diagram, the extrapolated lines for the invariant and pH-dependent regions intersect at pH = pK_a = 5.2.

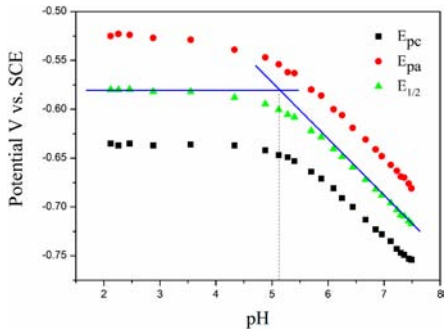

Figure 2. Peak potentials (E_{pc} and E_{pa}) and half-wave potential ($E_{1/2}$) vs pH in aqueous solution of $pyrH^+$ on a polished Pt electrode.

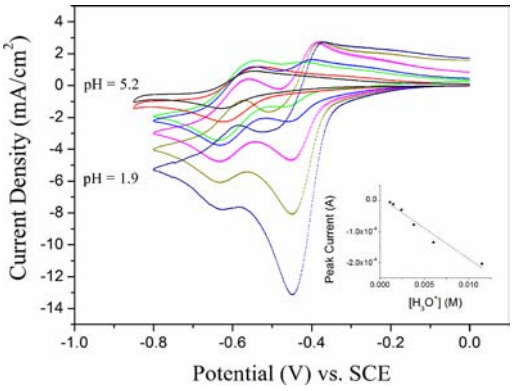

Figure 3. Separate processes for $pyrH^+$ and H_3O^+ reduction were observed in CV of 10 mM pyr at 100 mV/s at pH 1.9, 2.2, 2.4, 2.6, 2.8, 3.6, and 5.2. When pH < pK_a of $pyrH^+$, i_p was constant due to unchanging $[pyrH^+]$. At pH = pK_a = 5.2, i_p was reduced by half due to the lower $[pyrH^+]$. The H_3O^+ reduction wave appeared at sufficiently high $[H_3O^+]$ (∼1 mM, pH 3), and i_p increased linearly with $[H_3O^+]$ (inset).

To understand the effect of pK_a on the potential of catalysis we obtained reversible CV redox waves for >20 weak acids of varying structure: $pyrH^+$ derivatives, aromatic and nonaromatic acids such as amines, phenols, carboxylic acids, etc. (Table S1). The plateau $E_{1/2}$'s were measured and plotted versus their pK_a's (Figure 4). A linear relationship was readily obtained with slope ∼ −61 mV. Extrapolated to pH 0, this line intersected the

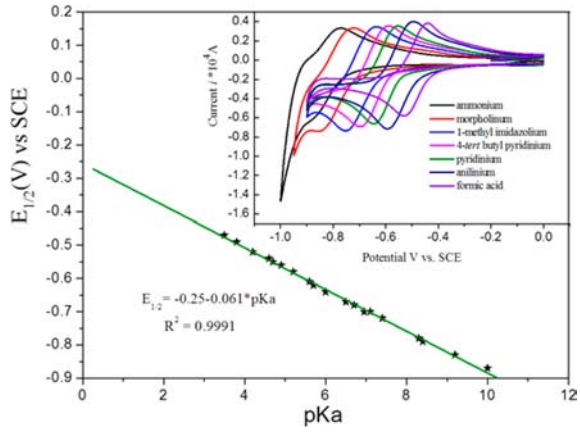

Figure 4. $E_{1/2}$ vs pK_a of weak acids in aqueous solution on a Pt disc electrode. Inset: CV of typical weak acids reduction on an alumina-polished Pt electrode in 0.5 M KCl aqueous solution at pH 3.4 (for each acid pH < pK_a and scan rate = 100 mV/s).

dx.doi.org/10.1021/ja4064052 | J. Am. Chem. Soc. 2013, 135, 14020−14023

potential axis at −0.25 V vs SCE, in good agreement with the standard hydrogen redox potential (−0.24 V vs SCE). This experiment clearly indicated that π-orbital reduction is not necessary to observe reversible waves on a Pt electrode. Any weak acid with a suitable pK_a results in an analogous redox wave. Fittingly, pyrH$^+$ follows this weak acid reduction trend, with an observed redox potential of −0.58 V vs SCE and a calculated redox potential of −0.57 V vs SCE at pK_a = 5.2 from the weak acid reduction equation:

$$E_{1/2} = -0.061\mathrm{p}K_a - 0.25 \qquad (3)$$

This experimentally obtained equation can be readily thermodynamically derived for proton reduction from a weak acid (eq 4) by combining eqs 4a−4c. This equation explains the general weak acid reduction on Pt electrodes in aqueous solution. Similar relationships were derived in studies of pK_a vs reduction potential of weak acids on Pt electrodes in aqueous,[21] organic,[22] and ionic liquid media.[23]

$$H_3O^+ + e^- \rightleftharpoons H_{(Pt)} + H_2O$$

$$E_{H^+/H_{(Pt)}} = -(G_{H_{(Pt)}} + G_{H_2O} - G_e - G_{H_3O^+})/nF \qquad (4a)$$

$$HA + H_2O \rightleftharpoons H_3O^+ + A^-$$

$$G_{A^-} + G_{H_3O^+} - G_{H_2O} - G_{HA} = -RT \ln K_a = 2.303RT\ \mathrm{p}K_a \qquad (4b)$$

$$HA + e^- \rightleftharpoons H_{(Pt)} + A^-$$

$$E_{HA/H_{(Pt)},A^-} = -(G_{H_{(Pt)}} + G_{A^-} - G_e - G_{HA})/nF \qquad (4c)$$

$$E_{HA/H_{(Pt)},A^-} = E_{H^+/H_{(Pt)}} - (0.059/n)\mathrm{p}K_a \qquad (4)$$

Based on the data presented here, pyrH$^+$ π-orbital-based reduction does not occur at a Pt electrode, but the importance of this reduction pathway should not be ignored for other pyrH$^+$ derivatives. For example, bpy can be reduced to form a π-radical species (Figure S1). For aromatic weak acids on a Pt electrode, two different reduction pathways are thus possible (Figure S6): reduction of proton to a surface hydride and π-system reduction. The π-system reduction may be favored at electrode materials where proton reduction is kinetically unfavorable.

In conclusion, we have experimentally investigated the mechanisms proposed to explain the pyridinium redox potential discrepancy between electrochemical observations and theoretical calculations. The intermediates of bpy and DHP suggested by Carter's group and surface-adsorbed pyrH$^+$ or pyrH$^\bullet$ by Musgrave's and Carter's groups are not strongly supported by the available experimental evidence. However, pyrH$^+$ reduction unambiguously follows the trend of any other weak acid's reduction at a Pt electrode as given by eq 4. This pathway is consistent with Batista group's theoretical insight into the formation of an interfacial Pt-H for the initial step of pyrH$^+$ reduction. Batista further suggested that the surface Pt-H then reduces a CO_2 that is H-bonded to a pyrH$^+$ species via the CO_2 oxygen.[12b] This aspect of the mechanism cannot be interrogated electrochemically, and we are devising spectroscopic tools to further probe the reaction dynamics. An intriguing alternative to Batista's proposal is a mechanism that utilizes the surface hydride to carry out a proton-coupled hydride transfer to an equilibrium carbamate formed between CO_2 and pyr.

■ ASSOCIATED CONTENT

Ⓢ Supporting Information

Experimental details and spectral data. This material is available free of charge via the Internet at http://pubs.acs.org.

■ AUTHOR INFORMATION

Corresponding Author

bocarsly@princeton.edu

Notes

The authors declare no competing financial interest.

■ ACKNOWLEDGMENTS

We acknowledge support by the Air Force Office of Scientific Research through the MURI program under AFOSR Award No. FA9550-10-1-0572 and NSF under Grant No. CHE-0911114. E.L.Z. acknowledges support in part by the Department of Energy Office of Science Graduate Fellowship Program, made possible by the American Recovery and Reinvestment Act of 2009, administered by ORISE-ORAU under Contract No. DE-AC05-06OR23100. We thank Dr. Paolo Stufano for helpful discussions.

■ REFERENCES

(1) Barton, C. E.; Lakkaraju, P. S.; Rampulla, D. M.; Morris, A. J.; Abelev, E.; Bocarsly, A. B. *J. Am. Chem. Soc.* **2010**, *132*, 11539.

(2) Seshadri, G.; Lin, C.; Bocarsly, A. B. *J. Electroanal. Chem.* **1994**, *372*, 145.

(3) Barton, E. E.; Rampulla, D. M.; Bocarsly, A. B. *J. Am. Chem. Soc.* **2008**, *130*, 6342.

(4) Bocarsly, A. B.; Gibson, Q. D.; Morris, A. J.; L'Esperance, R. P.; Detweiler, Z. M.; Lakkaraju, P. S.; Zeitler, E. L.; Shaw, T. W. *ACS Catal.* **2012**, *2*, 1684.

(5) de Tacconi, N. R.; Chanmanee, W.; Dennis, B. H.; MacDonnell, F. M.; Boston, D. J.; Rajeshwar, K. *Electrochem. Solid State* **2011**, *15*, B5.

(6) (a) Lee, K. Y.; Kochi, J. K. *J. Chem. Soc., Perkin Trans. 2* **1992**, 1011. (b) Yasukouchi, K.; Taniguchi, I.; Yamaguchi, H.; Shiraishi, M. *J. Electroanal. Chem. Interfacial Electrochem.* **1979**, *105*, 403.

(7) Morris, A. J.; McGibbon, R. T.; Bocarsly, A. B. *ChemSusChem* **2011**, *4*, 191.

(8) Kamrath, M. Z.; Relph, R. A.; Johnson, M. A. *J. Am. Chem. Soc.* **2010**, *132*, 15508.

(9) (a) Keith, J. A.; Carter, E. A. *J. Am. Chem. Soc.* **2012**, *134*, 7580. (b) Keith, J. A.; Carter, E. A. *J. Chem. Theory Comput.* **2012**, *8*, 3187.

(10) Lim, C.-H.; Holder, A. M.; Musgrave, C. B. *J. Am. Chem. Soc.* **2013**, *135*, 142. This mechanism is expected to be very surface sensitive. Consistent with this mechanism, we find changes in the CV response as the electrode material is changed (Au, C, Ni, and In have been screened). However, only the (111) Pt surface has been considered theoretically at this point; thus, it is not possible to evaluate our experimental data against a quantitative theoretical prediction.

(11) Keith, J. A.; Carter, E. A. *Chem. Sci.* **2013**, *4*, 1490.

(12) (a) Tossell, J. A. *Comp. Theor. Chem.* **2011**, *977*, 123. (b) Ertem, M. Z.; Konezny, S. J.; Araujo, C. M.; Batista, V. S. *J. Phys. Chem. Lett.* **2013**, 745.

(13) (a) Rüssel, C.; Jaenicke, W. *Electrochim. Acta* **1982**, *27*, 1745. (b) Eisner, U.; Gileadi, E. *J. Electroanal. Chem. Interfacial Electrochem.* **1970**, *28*, 81.

(14) Cole, E. B. Ph.D. Thesis, Princeton University, 2009.

(15) Wöß, E.; Monkowius, U.; Knör, G. *Chem.—Eur. J.* **2012**, *19*, 1489.

(16) Leopold, K. R.; Haim, A. *Inorg. Chem.* **1978**, *17*, 1753.

(17) Bard, A. J.; Faulkner, L. R. *Electrochemical Methods: Fundamentals and Applications*, 2nd ed.; John Wiley and Sons, Inc.: New York, 2001.

(18) Tanner, D. D.; Yang, C. M. *J. Org. Chem.* **1993**, *58*, 1840.

(19) O'Keane, J. Ph.D. Thesis, University of Glasgow, 1971.

(20) Costentin, C.; Robert, M.; Savéant, J. M. *Chem. Rev.* **2010**, *110*, PR1.

(21) Barrette, W. C.; Johnson, H. W.; Sawyer, D. T. *Anal. Chem.* **1984**, *56*, 1890.

(22) Kurek, S. S.; Laskowska, B. J.; Stokłosa, A. *Electrochim. Acta* **2006**, *51*, 2306.

(23) Barhdadi, R.; Troupel, M.; Comminges, C.; Laurent, M.; Doherty, A. *J. Phys. Chem. B* **2012**, *116*, 277.